J Bioenerg Biomembr (2011) 43:465–471
DOI 10.1007/s10863-011-9372-5

The nucleotide-binding domain 2 of the human transporter protein MRP6

Angela Ostuni · Rocchina Miglionico · Magnus Monné · Maria Antonietta Castiglione Morelli · Faustino Bisaccia

Received: 6 April 2011 / Accepted: 13 June 2011 / Published online: 12 July 2011

Abstract Multidrug-resistance-associated protein 6 (MRP6/ABCC6) belongs to the ABC transporter family, whose members share many characteristic features including membrane domains and two nucleotide-binding domains (NBD1 and NBD2). These function cooperatively to bind and hydrolyze ATP for the transport of substrates across biological membranes. In this study, MRP6-NBD2 (residues 1252–1503) was expressed in *Escherichia coli*, purified and structurally and functionally characterized. CD spectra suggested that the protein is folded. Furthermore, NBD2 is shown to be biologically active as it binds ATP and presents ATPase activity although significantly lower compared with isolated NBD1. The mixture of NBD2 and NBD1 exhibited an activity similar to the NBD2 alone, indicating that NBD1 and NBD2 form a heterodimer with the latter limiting ATP hydrolysis. These findings suggest that NBD1 has a higher tendency to form an active homodimer, which is also supported by in silico analysis of energy-minimized dimers of the homology models of the two domains.

Keywords ABC proteins · ATP binding and hydrolysis · CD spectroscopy · Fluorescence spectroscopy · MRP6/ABCC6 (Multidrug Resistance Protein 6) · Nucleotide binding domain 2 · In silico analysis

A. Ostuni (✉) · R. Miglionico · M. Monné · M. A. Castiglione Morelli · F. Bisaccia
Department of Chemistry "Antonio Mario Tamburro", University of Basilicata,
viale Ateneo Lucano 10,
85100 Potenza, Italy
e-mail: angela.ostuni@unibas.it

Introduction

Multidrug resistance protein MRP6 belongs to the superfamily of ABC transport proteins (Linton 2007). These transporters function as energy-dependent efflux pumps controlled by the ATP hydrolysis.

The MRP6 protein, like other ABC proteins, consists of two transmembrane domains and two cytoplasmatic nucleotide-binding domains (NBDs) characterized by the presence of Walker A, Walker B and ABC signature consensus sequences. MRP6 also contains an additional N-terminal transmembrane domain and an extracytosolic N-terminus. In addition to the full-length transcript of the ABCC6 gene, an alternatively spliced variant of ABCC6 that lacks exons 19 and 24 has been identified, thus yielding a splice variant that is distributed differently in various human tissues and cell lines (Armentano et al. 2008).

MRP6 plays an important physiological role as demonstrated by the fact that mutations in this gene cause Pseudoxanthoma elasticum (PXE) in humans, a recessive genetic disorder affecting connective tissues characterized by progressive mineralization of elastic fibers with pleiotropic consequences for ocular, vascular and other soft connective tissues (Finger et al. 2009). ABCC6 is expressed mainly in the liver and kidneys. Interestingly, tissues that are primarily affected in PXE express only low amounts of MRP6 (Kool et al. 1999). Therefore, the characterization of the mechanism of action of MRP6 and the identification of its physiological substrate, are important to understand the role of MRP6 in the physiopathology of PXE.

There is presently no crystallographic information about MRP6. High-resolution X-ray crystal structures of bacterial ABC transporters, together with the structures of a number of isolated NBDs crystallized in several nucleotide binding conditions, have provided a structural basis to discuss ATP

hydrolysis and transport by ABC transporters. The NBDs contain characteristic structural motifs responsible for the nucleotides binding and ATPase activity. The Walker A and Walker B conserved motifs are crucial elements for the nucleotide binding region to which the H-loop and the Q-loop also belong. The D-loop is involved in the intermolecular interactions at the NBD dimer interface and the C-motif of one NBD completes the nucleotide binding site of the other subunit (Smith et al. 2002; Locher et al. 2002; Zaitseva et al. 2005). Two identical catalytic sites were formed at the interface between two identical NBDs arranged in a head-to tail orientation (Smith et al. 2002; Locher et al. 2002). In the heterodimeric orientation the signature motif of one NBD is juxtaposed against the Walker A motif of the other.

Several studies have been carried out on isolated NBD1 of MRP1, which is homologous and exhibit a similar substrate specificity with MRP6 (Belinsky et al. 2002; Ilias et al. 2002). It has been reported that the two NBDs of MRP1 were not equivalent in ATP hydrolysis: NBD1 mainly serves a regulatory role through its binding to ATP, while NBD2 actually hydrolyzes ATP during the transport cycle of MRP1 (Chang 2007; Ramaen et al. 2003; Ramaen et al. 2005). The X-ray structure of MRP1-NBD1 has identified the residues involved in ATP binding and the residues that are potentially involved in ATP hydrolysis (Ramaen et al. 2006).

A homology model of human ABCC6, based on the Sav1866 crystal coordinates, showed a clustered distribution of the PXE-associated missense mutations in the predicted ABCC6 structure thus suggesting that domain–domain interactions are essential in the function of the transporter (Fülöp et al. 2009). Moreover, as in the other ABC transporters, MRP6-NBDs should be in close proximity to each other to reflect the previously described "nucleotide sandwich dimer" (Smith et al. 2002).

In order to elucidate the intrinsic properties of MRP6-NBDs and to relate its function in the full-length transporter we have started a systematic study on the structure and function of NBDs of ABCC6. Previously fluorescence and circular dichroism (CD) spectroscopic studies, together with ATP hydrolysis data of two polypeptides corresponding to residues from Asp-627 to Leu-851 and from Arg-648 to Thr-805 of the NBD1 region of MRP6, with and without some key residues for nucleotide binding and ATP hydrolysis, have been reported (Ostuni et al. 2010).

In this study, CD spectroscopy as well as ATP binding and ATPase activity assays were performed with MRP6-NBD2. The main results obtained show that the hydrolytic properties of NBDs of MRP6 are different and the ATPase activity of the heterodimer is similar to that of the NBD2 homodimer. The ATPase activities of isolated MRP6-NBD2 and in a mixture with NBD1 have been compared and evaluated by structural analysis of homology models of the NBDs.

Materials and methods

PCR amplification and construction of recombinant NBD2 expression vectors

The human ABCC6 cDNA sequences from base 3906 to 4427 or 3756 to 4509, respectively coding for the MRP6 protein sequence from Val-1295 to Arg-1468 or Thr-1252 to Val-1503, were amplified by PCR from the expression vector pcDNA3.1-ABCC6 (Armentano et al. 2008). In order to generate pQE3-NBD2$_{3906–4427}$, the forward primer 5′- TCGCGGATCCGTGGGCATCGTTGGCAGGA-3′ and the reverse primer 5′- CGAAAGCTTTCACCGGGCACA GTCCATCA-3′ were used. To construct pQE3-NBD2$_{3756–4509}$, the forward primer 5′-TCGCGGATCCACATGTGCAGCT CAGCCC-3′ and the reverse primer 5′-CGAAAGCTTTCA GACCAGGCCTGACTC-3′ were used. In both cases the NBD2 cDNA was cloned into pQE30 (Novagen) as a BamHI-HindIII restricted fragment.

Amplification was carried out in a 50 µl reaction volume containing 10 ng of template, 0.4 mM of each primer, 0.4 mM dNTPs, 2.5 mM $MgCl_2$, 2.5 units of Taq polymerase (Euroclone, CELBIO) and PCR buffer supplied with the enzyme. The PCR reaction was carried out on a THERMOHYBAID PCR System. The PCR reaction mixture was initially denatured at 95 °C for 2 min followed by amplification using 30 cycles of denaturation (45 s at 95 °C), annealing (58 °C for 1 min) and extension (1 min at 72 °C) with the final extension lasting 10 min. The PCR product was revealed on a 1% agarose gel, and the band corresponding to the desired PCR product was purified from the gel using a MinElute Gel Extraction Kit (Qiagen). The sequence and the correct orientation of the insert were confirmed by DNA sequencing (MWG-Biotech).

Expression and purification of NBD2 polypeptides

The recombinant vectors were used to transform BL21DE3 (Stratagene) cells. The pQE30 vectors allow the expression of an N-terminal His-tagged fused NBD2. The transformants were selected on Luria Bertani (LB) plates containing 100 µg/mL ampicillin. Single colonies of transformed strains were grown overnight in 2 mL of LB supplemented with antibiotic at 37 °C, before being diluted 1:100 into selective media. Growth was continued at 37 °C until an OD600 of 0.6–0.8 was attained and protein expression was induced by the addition of isopropyl-thiogalactoside (IPTG) to a final concentration of 0.1 mM. Growth was continued for 5 h, then cells were harvested by centrifugation at 4 °C for 15 min at 10000 rpm, and pellets retained at −20 °C until required. Bacterial cell pellets were resuspended in lysis buffer (1 mM phenylmethylsulfonyl fluoride, PMSF, 25 mM Tris, 300 mM NaCl, pH 8) and lysed by repeated 10 s bursts of sonication on

ice (Bandelin sonicator). Cell lysates were clarified by centrifugation at 10000 rpm for 15 min at 4 °C. Protein fractions were analyzed on 15% SDS–polyacrylamide gels and after electroblotting, the polyvinylidene difluoride (PVDF) membranes were treated with Monoclonal Anti-polyHistidine-Peroxidase antibody (Sigma). The immuno-reaction was detected by the peroxidase reaction performed with 20 mL of a mixture of 4-chloro-1-naphthol (0.05% w/v), methanol (16% v/v), and bovine serum albumin (0.5% w/v) in a medium containing 0.14 M phosphate (pH 7.0) with the final addition of 10 mL of 30% H_2O_2.

The supernatant of the cell lysate was applied onto a 5 ml Ni NTA HIS BIND RESIN (Novagen) column equilibrated with a buffer containing 25 mM Tris/HCl, pH 8.0, 300 mM NaCl, 10 mM imidazole. After shaking at 4 °C for 5 h and washing with a buffer 50 mM Tris/HCl, pH 8.0, 300 mM NaCl, 20 mM imidazole (5 column volumes), the bound fraction was eluted with the buffer containing 250 mM imidazole. After dialysis in double distilled water and lyophilization, further purification of NBD2 polypeptides was obtained by reverse-phase VP 250/10 NUCLEOSIL 300-7- C4 column Macherey-Nagel using a gradient of acetonitrile/water in 0.1% trifluoroacetic acid.

Protein concentration was determined by measuring the optical absorbance at 280 nm using an extinction coefficient calculated from the amino acid composition: 18240 M^{-1} cm^{-1} (s-NBD2) or 26720 M^{-1} cm^{-1} (l-NBD2).

Circular Dichroism spectroscopy

The CD spectra were acquired at 25 °C with a Jasco J-815 Circular Dichroism Spectrometer equipped with a thermoelectric temperature controller, using a 0.1 cm cylindrical quartz cuvette. Spectra of l-NBD2 were obtained in 25 mM Tris/HCl (pH 8), 100 mM NaCl and 10 mM $MgCl_2$ or in 70% trifluoroethanol (TFE) with 0.1 nm-steps from 190 to 250 nm, 1 nm bandwidth, a time-constant of 0.5 s and 20 mdeg of sensitivity. After the baseline spectra of the solvents were subtracted, spectra were smoothed using the Fourier transform routine of the J-815. Data were expressed in terms of the molar ellipticity per residues $[\theta]_{RMW}$ in units of degxcm^{2}xdmol^{-1}. Analysis of CD spectra for the evaluation of secondary structure content was performed with DICHROWEB using the algorithm CONTINLL (van Stokkum et al. 1990).

Intrinsic Fluorescence measurements

Binding of ATP and ADP to l-NBD2 was monitored by changes in the intrinsic tyrosine/tryptophan fluorescence of the polypeptide. The experiment was performed at 25 °C on a Fluorog-3 spectrometer (Jobin Yvon/SPEX instrument). To determine the dissociation constants of the interaction, aliquots of ATP and ADP, in concentrations ranging from 0.05 to 2 mM, were added to a 1 μM solution of each polypeptide in a buffer containing 25 mM Tris/HCl (pH 8), 100 mM NaCl and 10 mM $MgCl_2$. All data collection was performed with DATAMAX software. The spectra were corrected for background fluorescence from the buffer. The excitation wavelength was set at 278 nm and emission was scanned over the range 300–400 nm. The fluorescence at 340 nm was measured. The experimental results were plotted using SIGMAPLOT 11 software and a single nucleotide-binding site model as fit function (Hovius et al. 2000).

ATPase activity assay

The ATPase activity of l-NBD2 polypeptide was determined by using the EnzChek phosphate Assay Kit (Invitrogen), a colorimetric method, to measure the release of inorganic phosphate by 2 μM of purified polypeptide incubated for 1 h at 37 °C in a buffer containing 25 mM Tris/HCl (pH 8), 100 mM NaCl, 10 mM $MgCl_2$ and 4 mM ATP. A sample containing only 4 mM ATP was incubated in parallel for 1 h at 37 °C, to correct for spontaneous hydrolysis. The absorbance was read at 360 nm after 1 h incubation at 22 °C in presence of 2-amino-6-mercapto-7-methylpurine ribonuleoside and purine-nucleoside phosphorylase (purine-nucleoside:orthophosphate-ribosyltransferase, EC 2.4.2.1). The ATPase activity is expressed as phosphate nmoles × (polypeptide nmoles)$^{-1}$ × hour^{-1}.

Homology modeling and structural analysis

The models of the NBDs of human MRP6 were constructed by using the structures of the closest sequence homologues in PDB as templates for Modeller (Fiser and Sali 2003): human NBD1 of MRP1 (PDB ID 2CBZ) has 50% sequence identity with MRP6-NBD1 (Ramaen et al. 2006) and NBD2 of CFTR (PDB ID 3GD7) is 43% identical with MRP6-NBD2 (Atwell et al. 2010). The alignments were done with ClustalW in STRAP (Gille and Frömmel 2001). For the creation of the dimer models, the domains were superimposed on the homodimer of CFTR NBD1 (PDB ID 2PZE) by using PyMol (Schrödinger, www.pymol.org) and the positions of ATP within this structure were used as templates for the substrates ADP and ATP. The models were energy optimized by the YASARA energy minimization server (Krieger et al. 2009) and evaluated by PISA (Krissinel and Henrick 2007).

Results and discussion

Production and purification of the NBD2 polypeptides

In order to characterize MRP6-NBD2, two polypeptide chains were originally generated from Val-1295 to Arg-

1468 (s-NBD2) and from Thr-1252 to Val-1503 (l-NBD2) (Fig. 1). The MRP6-NBD2 were expressed in a bacterial expression system. The pQE30 vector was chosen to overproduce NBD2 in *E. coli* as an N-terminally His_6-tagged protein. Thus, in the construct a short sequence of 12 amino acids, MRGSHHHHHHGS, is added at the N-terminus. The boundaries of s-NBD2 within the complete MRP6 sequence, encoded by exons 28, 29 and 30, have been defined as reported by (Le Saux et al. 2001) but it was scarcely soluble to be used for structural and functional studies. The construct l-NBD2 has been defined by homology with MRP1-NBD2 and it is the subject of this study (hereafter it will be mentioned only as NBD2).

As shown in Fig. 2, upon induction by IPTG, NBD2 was expressed as a major protein product (Fig. 2a, lane 3) compared to the uninduced bacterial cultures (Fig. 2a, lane 2). The polypeptide was found to form mainly insoluble inclusion bodies (Fig. 2a, lane 4) while only a smaller fraction of the expressed protein was localized in the bacterial cytoplasm (Fig. 2a, lane 5). The optimal yields were achieved when bacteria were grown at 37 °C, and harvested 5 h after 0.1 mM IPTG induction. The soluble fractions of the cell lysates were purified in two stages: first on a Ni-NTA resin, eluted with a buffer of 250 mM imidazole (Fig. 2a, lane 6) and then further purified by RP-HPLC (Fig. 2a, lane 7).

Circular dichroism spectra

To obtain information about secondary structure of NBD2, circular dichroism spectra of the polypeptide were recorded at 25 °C. The experiments were performed with a buffer containing 25 mM Tris/HCl (pH 8), 100 mM NaCl and 10 mM $MgCl_2$ and in mixtures of water and TFE (70% v/v) (Fig. 3). TFE is a cosolvent that is used to probe helical propensity as it is believed to stabilize secondary protein structures, in particular, helical conformation and β-hairpins (Shiraki et al. 1995). Evaluation of the secondary structure content performed with DICHROWEB using the algorithm CONTINLL showed that polypeptide Thr-1252 to Val-1503 is highly structured. As indicated by two characteristic minima at 208 and 220 nm, the polypeptide assumes predominantly an α-helical conformation in TFE solution. On the contrary, in saline buffer, the polypeptide presents a mixture of secondary structures: 27% helix, 34% strand and 39% turns.

Fluorescence measurements of nucleotide binding to the polypeptide

Fluorescence quenching experiments were performed to measure nucleotide binding. A decrease in intrinsic fluorescence of the polypeptide at 340 nm was observed in the titrations with ATP and ADP. Fig. 4 shows the maximum quenching of fluorescence at 340 nm after saturation of the polypeptide with nucleotides using λ excitation for the tyrosine/tryptophan chromophores at 278 nm. The experimental results were plotted using the SIGMAPLOT 11 software with a single nucleotide-binding site model as fit function. NBD2 binds nucleotides with a Kd in the same range as NBD1 (Ostuni et al. 2010). In particular, NBD2 bound ATP with a Kd (μM) of 208±18 and ADP with a Kd 259±15.

ATPase activity of the NBD2 polypeptide

To exclude any contamination from bacterial ATPase, we carried out two steps of purification of polypeptides after overexpression in *E.coli*. To determine the ATPase activity of the NBDs, we quantified spectrophotometrically the inorganic phosphate produced during the hydrolysis of 4 mM ATP by the heterodimer and/or homodimers incubated for 1 h at 37°. The production of Pi by NBD2 was 4±2 nmoles × (polypeptide nmoles)$^{-1}$ × hour^{-1}, lower than that exhibited by NBD1 (15±2 nmoles × (polypeptide nmoles)$^{-1}$ × hour^{-1}) (Ostuni et al. 2010). All data reflect

^{1252}TCAAQPPWPQGGQIEFRDFGLRYRPELPLAVQGVSFKIHAGEK

VGIVGRTGAGKSSLASGLLRLQEAAEGGIWIDGVPIAHVGLHTL

RSRISIIPQDPILFPGSLRMNLDLLQEHSDEAIWAALETVQLKALV

ASLPGQLQYKCADRGEDLSVGQKQLLCLARALLRKTQILILDEA

TAAVDPGTELQMQAMLGSWFAQCTVLLIAHRLRSVMDCARVLV

MDKGQVAESGSPAQLLAQKGLFYRLAQESGLV^{1503}

Fig. 1 MRP6-NBD2 polypeptide sequence. Polypeptide has been produced with a histidine-tag at the N-terminus, MRGSHHHHHHGS. The A-loop (*underlined*); the ATP-binding motifs (Walker-A and Walker-B, *double underlined* and *dotted wave-underlined* respectively), the Q loop (*point-underlined*), the ABC-signature sequence (*wave-underlined*), the D-loop (*bolded*) and the histidine loop (*point-line-underlined*) are indicated

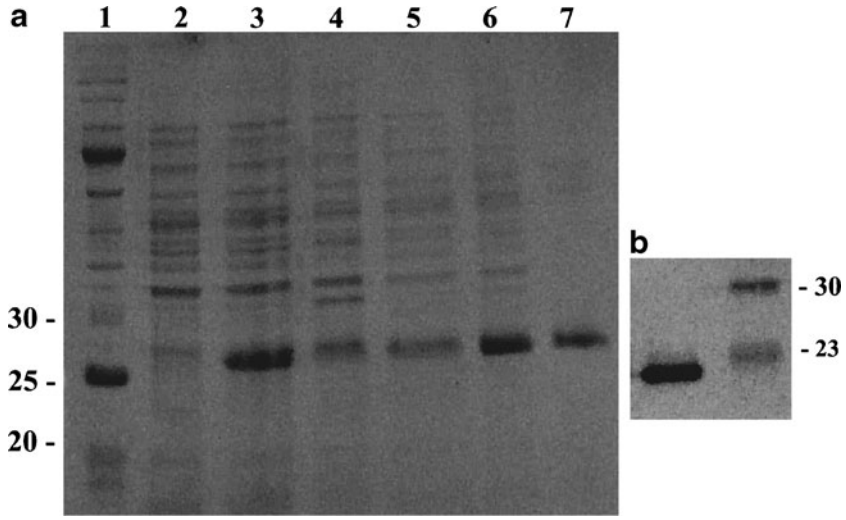

Fig. 2 Expression and purification of NBD2 polypeptide. **a** NBD2 polypeptide was purified as described in the Materials and Methods section and each purification step was analysed by SDS/PAGE (15% gel) and Coomassie Blue staining. *Lane 1*, protein molecular-mass standards (kDa); *lane 2*, total bacterial proteins before induction; *lane 3*, total bacterial proteins of IPTG-induced cells; *lane 4*, insoluble fractions after sonication; *lane 5*, soluble proteins after sonication; *lane 6*, polypeptide purified on nickel-chelating resin; *lane 7*, polypeptide purified by RP-HPLC. **b** NBD2 Western immunoblotting with Monoclonal Anti-polyHistidine-Peroxidase antibody

mean values±SD for 5 independent trials. The addition of NBD2 reduced the NBD1 hydrolytic activity to 5±2 nmoles × (polypeptide nmoles)$^{-1}$ × hour^{-1} thus suggesting the heterodimer formation.

Homology modeling

Homology models of MRP6-NBD1 and -NBD2 were created and the potential dimer and substrate combinations were simulated by using the structure of the CFTR-NBD1 homodimer as a template, which is thought to mimic the arrangement of the native heterodimer. This structure has previously been used as a framework to analyze the positions of mutations known to impede MRP6 activity (Fülöp et al. 2009). The dimer assemblies (Fig. 5) were evaluated by the PISA server (Table I). All different variations with ATP and ADP in one site or the other or in combination were evaluated but all results were very similar to what is presented in Table 1. It is striking that

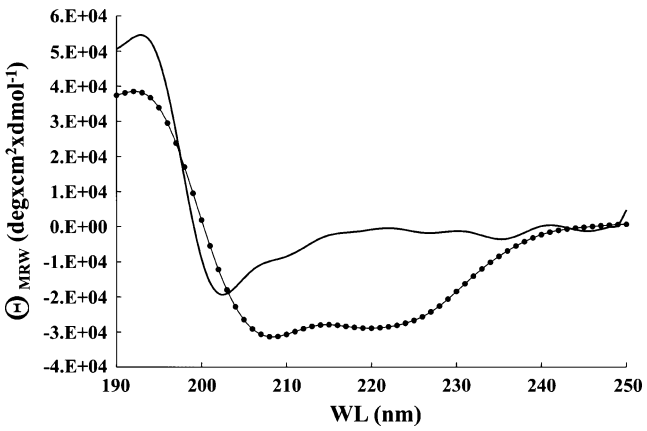

Fig. 3 CD spectra of NBD2 at 25 °C in 25 mM Tris/HCl (pH 8), 100 mM NaCl and 10 mM $MgCl_2$ (–) or in 70% TFE (*filled circle*). Data were expressed in terms of the molar ellipticity per residues $[\theta]_{RMW}$ in units of degxcm^{2}xdmol^{-1}

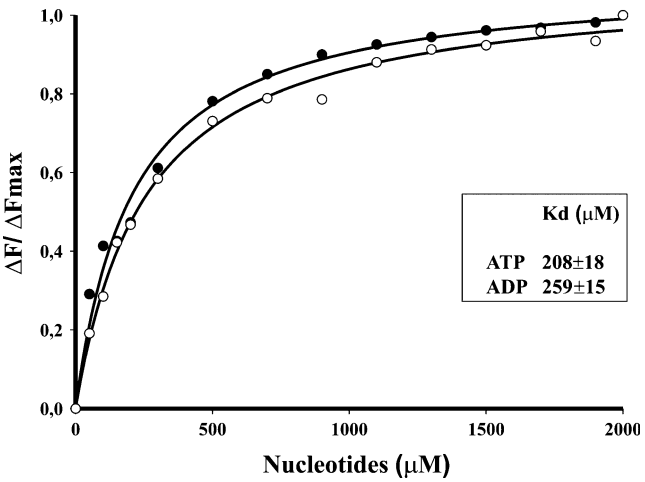

Fig. 4 Characterization of polypeptide-nucleotide interaction by intrinsic fluorescence. Maximum quenching of fluorescence at 340 nm obtained after saturation of NBD2 by ATP (*filled circle*) and ADP (*empty circle*). Experiments were performed at a polypeptide concentration of 1 μM and nucleotide concentrations ranging from 0.05 to 2 mM. Values are expressed as a percentage of the maximal peak fluorescence quenching, ΔF/ΔFmax. The dissociation constant Kd for the polypeptide-nucleotide complexes was determined from a single nucleotide-binding site model as fit function

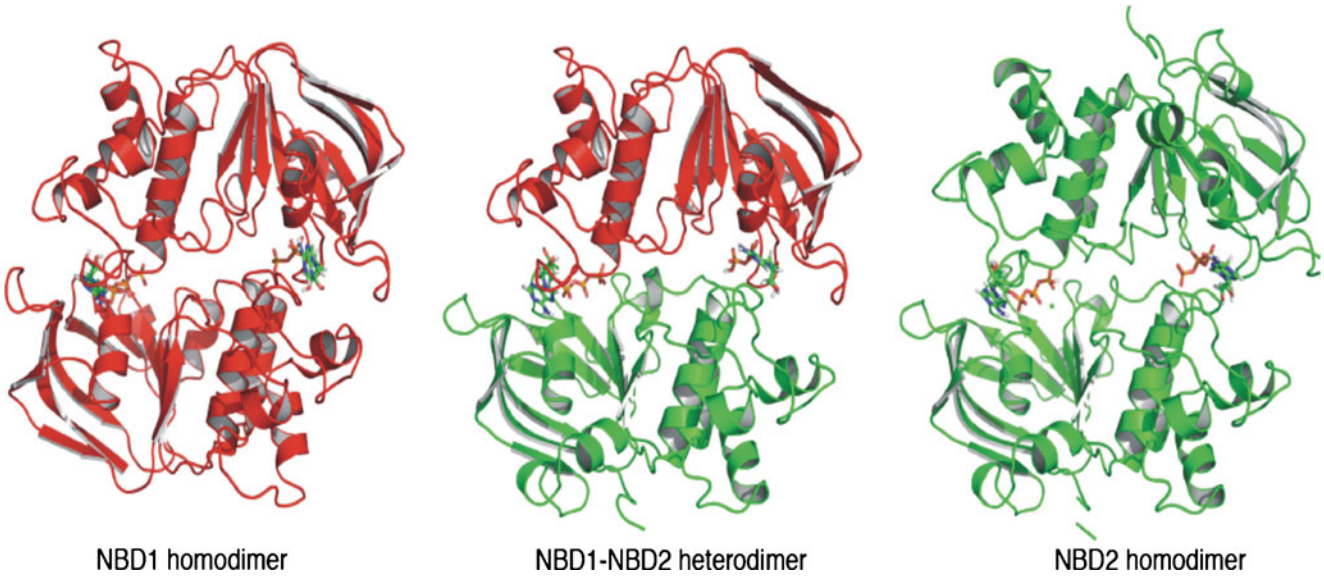

Fig. 5 Cartoon representation of the homology models of NBD1 (*red*) and NBD2 (*green*) assembled into homo- and hetero-dimers with ATP bound at the two binding sites

NBD1-NBD2 and NBD1-NBD1 dimers have negative $\Delta^i G$ values, on average, of about −7.6 and −6.5 kcal/mol, respectively, meaning that dimer formation is favored, while this is not the case for hypothetical NBD2-NBD2 dimers where $\Delta^i G$ is less than −0.1 kcal/mol. It could be argued that this is due to the fact that the dimer template is more similar to NBD1 (29% identity compared to 25% for NBD2) but, in that case, only NBD1 homodimers should be energetically favorable and not NBD1-NBD2 heterodimers. In fact, on average, the lower $\Delta^i G$ P-value of about 0.26 kcal/mol, for all NBD1-NBD2 indicates that these heterodimers are more likely to be interaction-specific than the NBD1 homodimer (0.40 kcal/mol) and the NBD2 homodimer (0.72 kcal/mol). Both may be considered an artifact although having more hydrogen bonds and salt bridges than the heterodimers thus indicating that the surfaces taking part in the interactions between NBD1 and NBD2 are more complementary. Taken together, this suggests that the NBD1-NBD2 heterodimer model is stable and, of course, it is also known to work in vivo. The formation of NBD1 homodimers are energetically favorable, potentially forming and being active in vitro, while NBD2 homodimers are not formed at all.

Conclusions

With the aim of understanding the action of the NBDs of MRP6, in the present work we have produced and characterized a polypeptide corresponding to the NBD2 (residues from Thr-1252 to Val-1503). Most of the studies on isolated NBDs from ABC transporters have

Table 1 In silico analysis of the stability of the homo- and hetero-dimers with ADP or ATP bound in the two binding sites by the PISA server

Dimer	Site A	Site B	Area (Å^2)	$\Delta^i G$ (kcal/mol)	$\Delta^i G$(P-value)	H-bonds	Salt bridges
NBD1-NBD2	ADP	ADP	705	−7.5	0.254	1	1
	ATP	ATP	655	−7.7	0.271	3	1
NBD1-NBD1	ADP	ADP	921	−6.3	0.414	4	3
	ATP	ATP	882	−6.8	0.388	5	2
NBD2-NBD2	ADP	ADP	660	0.3	0.734	4	9
	ATP	ATP	588	−0.4	0.715	5	10

The interface area is calculated as the difference in the total accessible surface areas of isolated and interfacing structures divided by two. The $\Delta^i G$ indicates the solvation free energy gain upon formation of the interface. The $\Delta^i G$ P-value indicates the probability of getting a lower $\Delta^i G$ if the interaction interface was picked randomly on the two molecules. $P>0.5$ means that the interface is probably an artifact and $P<0.5$ that the interface is likely to be interaction-specific. The number of hydrogen bonds and salt bridges are indicated.

been limited by the tendency of these proteins to form aggregates, however, the MRP6-NBD2, although with a low yield, was successfully expressed as a soluble protein in *E. coli*, and subsequently purified by Ni^{2+}-affinity chromatography and HPLC for structural and functional characterization.

The CD spectra demonstrate that NBD2 is highly structured in saline solution with a different contribution of α-helix, β-strand and turn conformations at equilibrium. Another evidence that NBD2 polypeptide is well folded derives from its capability to bind nucleotides with high affinity. The ATPase activity of NBD2 is lower with respect to NBD1. This could be explained by considering that NBD2, although appropriately folded, has a low propensity to assemble in a functionally active homodimer as also suggested by the in silico structural analysis. Moreover, the lower ATPase activity of the mixture NBD1-NBD2 compared with NBD1 alone indicates that NBD1 is interacting with NBD2 to produce a stable heterodimer. These findings might have implications for how ABC transporters work in vivo.

Even though homodimerization is not physiological in the full-length transporter, where NBD1 interacts with NBD2, this property is fundamental in half-transporters that work as homodimers (Shiraki et al. 1995). In this context, the different behaviors of NBD1 and NBD2 are interesting above all for ABC transporters that form half-transporters as a result of alternative splicing (Biemans-Oldehinkel et al. 2006).

The experimental and theoretical evidences presented here support the formation of an NBD1-NBD2 heterodimer with a low activity. This could be explained by the in vivo situation, where ATP is most likely hydrolyzed exclusively when substrate binding in the membrane domains leads to conformational changes that activates the NBDs. In the in vitro case, as presented here, the NBD1-NBD2 heterodimer is formed but it is not active because of the lack of the required conformational changes. In other words, the NBD1 homodimer presents an uncontrolled activity while the activity of the NBD1-NBD2 heterodimer is regulated.

References

Armentano MF, Ostuni A, Infantino V, Iacobazzi V, Castiglione Morelli MA, Bisaccia F (2008) Research Letters in Biochemistry. Article ID 912478, 4 pages, doi:10.1155/2008/912478

Atwell S, Brouillette CG, Conners K, Emtage S, Gheyi T, Guggino WB, Hendle J, Hunt JF, Lewis HA, Lu F, Protasevich II, Rodgers LA, Romero R, Wasserman SR, Weber PC, Wetmore D, Zhang FF, Zhao X (2010) Protein Eng Des Sel 23(5):375–384

Belinsky MG, Chen ZS, Shchaveleva I, Zeng H, Kruh GD (2002) Cancer Res 62:6172–6177

Biemans-Oldehinkel E, Doeven MK, Poolman B (2006) FEBS Lett 580(4):1023–1035

Chang XB (2007) Cancer Metastasis Rev 26(1):15–37

Finger RP, Charbel Issa P, Ladewig MS, Göttin C, Szliska C, Scholl HP, Holz FG (2009) Surv Ophthalmol 54(2):272–285

Fiser A, Sali A (2003) Methods Enzymol 374:461–491

Fülöp K, Barna L, Symmons O, Závodszky P, Váradi A (2009) Biochem Biophys Res Commun 379:706–709

Gille C, Frömmel C (2001) Bioinformatics 17(4):377–378

Hovius R, Vallotton P, Wohland T, Vogel H (2000) Trends Pharmacol Sci 21:266–273

Ilias A, Urban Z, Seidl TL, Le Saux O, Sinko E, Boyd CD, Sarkadi B, Varadi A (2002) J Biol Chem 277:16860–16867

Kool M, van der Linden M, de Haas M, Baas F, Borst P (1999) Cancer Res 59:175–182

Krieger E, Joo K, Lee J, Lee J, Raman S, Thompson J, Tyka M, Baker D, Karplus K (2009) Proteins 77(9):114–122

Krissinel E, Henrick K (2007) J Mol Biol 372(3):774–97

Le Saux O, Beck K, Sachsinger C, Silvestri C, Treiber C, Göring HH, Johnson EW, De Paepe A, Pope FM, Pasquali-Ronchetti I, Bercovitch L, Marais AS, Viljoen DL, Terry SF, Boyd CD (2001) Am J Hum Genet 69(4):749–764

Linton KJ (2007) Physiology 22:122–130

Locher KP, Lee AT, Rees DC (2002) Science 296:1038–1040

Ostuni A, Miglionico R, Castiglione Morelli MA, Bisaccia F (2010) Protein Pept Lett 17:861–866

Ramaen O, Masscheleyn S, Duffieux F, Pamlard O, Oberkampf M, Lallemand JY, Stoven V, Jacquet E (2003) Biochem J 376:749–756

Ramaen O, Sizun C, Pamlard O, Jacquet E, Lallemand JY (2005) Biochem J 391:481–490

Ramaen O, Leulliot N, Sizun C, Ulryck N, Pamlard O, Lallemand JY, Tilbeurgh H, Jacquet E (2006) J Mol Biol 359:940–949

Shiraki K, Nishikawa K, Goto Y (1995) J Mol Biol 245:180–194

Smith PC, Karpowich N, Millen L, Moody JE, Rosen J, Thomas PJ, Hunt JF (2002) Mol Cell 10:139–149

van Stokkum IH, Spoelder HJ, Bloemendal M, van Grondelle R, Groen FC (1990) Anal Biochem 191:110–118

Zaitseva J, Jenewein S, Jumpertz T, Holland IB, Schmitt L (2005) EMBO J 24:1901–1910